ELSEVIER

Materials Science and Engineering B56 (1998) 60–68

MATERIALS SCIENCE & ENGINEERING B

Graded and stacked thermoelectric generators—numerical description and maximisation of output power

L. Helmers *, E. Müller, J. Schilz, W.A. Kaysser

Institute of Materials Research, German Aerospace Center (DLR), D-51170 Cologne, Germany

Received 25 June 1998

Abstract

Large temperature differences applied to thermoelectric generators require that the variations of all material properties with temperature are included in a numerical description of their performance. A finite element algorithm is developed to calculate the temperature field in a thermoelectric device and concomitantly its thermoelectric performance under operation conditions. Spatially varying the composition of material or the doping concentration allows to enhance the power output or efficiency. The choice of the optimum concentration parameter profiles is shown not to be a function of the local temperature only, but to be dependent on a local criterion related to the entire temperature field. This criterion is included in an iterative calculus to find optimised concentration profiles. It is shown that the code developed has advantages over previously published solutions, since it can be applied to continuous and discontinuous material changes without any assumptions on the mutual dependence of the governing transport parameters or a need to cast their temperature dependence into analytical form. The performance is shown for some test situations and compared to literature.

Keywords: Finite element algorithim; Power output; Thermoelectric generators

1. Introduction

Thermoelectric generators are driven with large temperature differences to convert the heat flow through them into electric energy with high efficiency. In typical applications the difference across the thermoelectric material amounts to some 100 K. A temperature interval as large as this does not usually allow consideration of the material properties determining performance (i.e. Seebeck coefficient, thermal and electrical conductivity) as independent of temperature. Because of this fact, the constant property approach commonly used in the description of thermoelectric devices, [1], is always an approximation.

Several calculation approaches, that include the temperature dependence of the material properties, have been published in the literature, but there is always a need to express the temperature dependence analytically or even the mutual relationships between the material properties in order to reduce the number of parameters, [3,4,11]. In particular, none of the approaches are able to deal with arbitrary temperature dependencies of the material properties which include abrupt property changes as occurring in a stacked thermoelectric element (Fig. 1).

Here we present an exact and flexible procedure, based on a finite element approach. It is easy to use and needs only tabulated values of material parameters as input. There is no physical restriction on their temperature dependence. Both, continuous and discrete material transitions are correctly dealt with. Even artificial materials can be modelled, which offers the possibility to deal with the thermoelectric performance of quantum wells and other new materials.

Since the material parameters usually depend on the concentration of the dopants or the composition of the semiconductor, it has been suggested to exploit the concentrational dependence of one or more of the mentioned, temperature-dependent, transport properties to optimise the performance of the whole device

* Corresponding author.

0921-5107/98/$ - see front matter
PII S0921-5107(98)00211-6

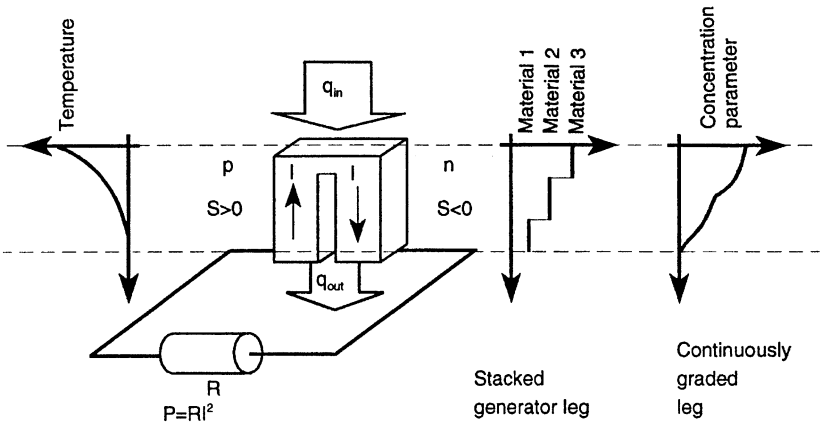

Fig. 1. A thermoelectric generator is typically operated in large temperature differences. Graded or stacked devices improve the performance by selecting the material in accordance with the temperature field.

[2,3]. The basic idea is indeed simple: If, in a one-dimensional description, the temperature field in a thermoelectric leg is known, one can in principle adjust the local composition in order to maximise the overall efficiency or output power of the device Fig. 1. However, any alteration of the compositional profile will change the temperature field inside the leg in response, which has to be taken into account in numerical considerations.

The maximisation itself, i.e. the calculation of the spatial material or compositional profile, has previously been performed by either testing discrete materials at spatial intervals [9], or selecting compositional profiles [3], out of a heavily restricted variety with only few (two or three) free coefficients, or by applying standard maximisation procedures to the assumed functional temperature dependence of the transport coefficients [5].

Our practical solution deals with this problem by an iteration of the sequence 'calculation of the temperature-field/selection of material'; where a new local criterion to select the material composition is used.

It will be shown, that the local choice of material always has to consider the whole thermal environment of each volume increment. In other words, the local contribution to the output power is not only a function of local temperature and composition, but depends on the temperature field throughout the device. This is in contrast to known concepts that focus on a 'local figure of merit', which may be defined by $Z = S^2 \cdot \sigma/\kappa$, ($S$, Seebeck coefficient; σ, electrical conductivity; κ, thermal conductivity). Here Z is a material property. Maximising Z at any place has no physical justification to maximise the power output or the efficiency. As a first evidence to this point, one can judge that Z is commonly introduced in the description of a constant property thermoelectric generator. In a generator with spatial variation of material (graded or stacked generator as sketched in Fig. 1) the situation is different: A thin slice, where the properties may be regarded to be constant, is not operated as a stand alone generator. The electric current passing through this single slice arises from thermovoltages produced by the whole stack of slices and is additionally determined by a load resistor, which is matched to the whole generator. The influence of the single slice on the integral current generation is only of the order $1/N$ (N, total number of slices). Thus the local contribution has to be a function of the whole thermovoltage collected and the outer load, which both are integral quantities.

The paper is arranged as follows: In Section 2 the finite element procedure for the temperature field calculation is introduced, which is the base to calculate the performance of an arbitrary thermoelectric generator. For practical applications it is of great interest to provide the optimum design for graded or stacked generators (i.e. continuous or discontinuous material changes). We combined the calculus for the temperature field with the procedure to select the concentration parameter, Section 3, and obtained suggestions for optimum device designs. Before presenting some results of device designs in the last chapter 6, the peculiarities of the inclusion of discontinuous material changes into the calculation are discussed, Section 4. In Section 5 the use of this approach as a design tool is discussed and compared with the literature.

2. Calculating the temperature field

The temperature field inside a thermoelectric generator can be derived from the known set of coupled integral differential equations, [6]:

$$0 = \nabla \cdot (k \nabla T) - Ti \cdot \nabla S + \rho i^2 = D([T(x)]), \tag{1}$$

$$i = -ej = \int_0^L \mathrm{d}x \, \frac{S \nabla T}{\left(\tilde{R} + \int_0^L \mathrm{d}x \, \rho \right)}. \tag{2}$$

Table 1
Terminology used throughout this article

Symbol	Quantity	Unit	Fundamental relation
x	Spatial coordinate	m	
T	Temperature	K	
s	Flux of entropy	J K^{-1} s^{-1} m^{-2}	
u	Flux of energy	J s^{-1} m^{-2}	
n	Density of particles	m^{-3}	
$\boldsymbol{j}$	Flux of particles	s^{-1} m^{-2}	
i	Electric flux	C s^{-1} m^{-2}	
ϕ	Electrostatic potential	J C^{-1}	
σ	Electric conductivity	Ω^{-1} m^{-1}	
ρ	Electric resistivity	Ω m	$\rho = \sigma^{-1}$
κ	Thermal conductivity	W K^{-1} m^{-1}	
S	Seebeck coefficient	V K^{-1}	
q	Heat flux	J s^{-1} m^{-2}	$\mathbf{q} = T \cdot \mathrm{s}$
$\tilde{R}$	Load resistance/generator cross sectional area	Ω m^{-2}	R/A
μ	Energetic potential of the charge carriers	J	

(For the meaning of the symbols refer to Table 1.) These equations state the conservation of energy and number of charge carriers as well as linear transport obeying the Onsager relations.

To solve Eq. (1), we apply an iterative approach to take the integral character of Eq. (2) into account. This allows to treat the coefficients of Eq. (1) just as functions of temperature, but independent of the whole temperature field. We restrict the solution to one-dimensional fields, i.e. $T = T(x)$, etc. because we focus on large temperature differences along the axis of a thermogenerator. If there are transverse differences, they are due to inhomgeneous heat flux at the hot or cold junction of the material or due to radiation losses. Typical devices are designed to have isothermal junctions, therefore any transverse temperature variation will be much smaller than the axial one.

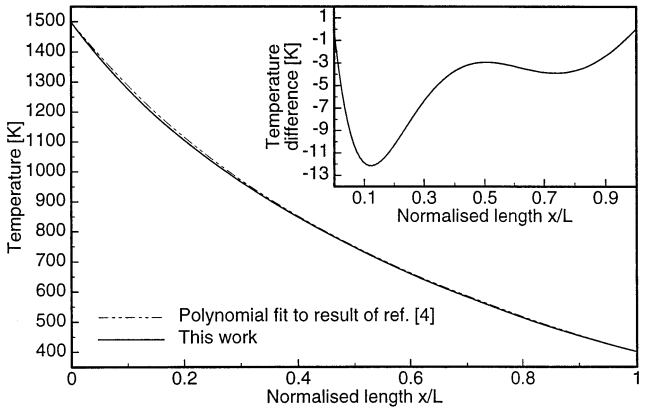

Fig. 2. Temperature profile in the n-leg of a thermoelectric generator. The temperature dependent material properties were introduced by Sherman et al. [4]. Within the precision of the results available from Ref. [4] the results match perfectly. The inset shows the remaining difference between both profiles.

Thermoelectric devices are generally assembled forming pairs of p and n-type material, the p- and n-leg with positive and negative Seebeck coefficients, respectively, Fig. 1. Often such a couple is treated as a unit [4], where both, the p and the n-leg, are included in the calculus. But it is sufficient for a comprehensive characterisation and optimisation, to treat the legs individually. It can be shown, that optimised conditions require a matched electric current density. When combining the two legs to the desired thermocouple, the respective current densities in the two materials have to be conserved by adjusting the area ratio of the legs and combining the two calculated load resistances.

Under these conditions a one dimensional temperature field is calculated using a direct solution according to Galerkin's method of the finite element algorithm (e.g. [7,8]). We used equidistant, linear element functions $f_i(x)$ along the material. The temperature field thus has the following representation:

$$T(x) = \sum_{i, x \in [0,L]} T_i f_i(x). \tag{3}$$

Table 2
Design of a stacked generator. 3 (2) hypothetical, constant property materials are combined to form the p (n-)leg, resp., of a generator

Material designation	Temperature range [K]	Relative length of the segment	
		Reference [11]	This work
P1	880…720	0.551	0.575
P2	720…420	0.291	0.280
P3	420…300	0.158	0.145
N1	880…420	0.772	0.795
N2	420…300	0.228	0.205

The results of Ref. [11], who have proposed the material properties, are close to this approach.

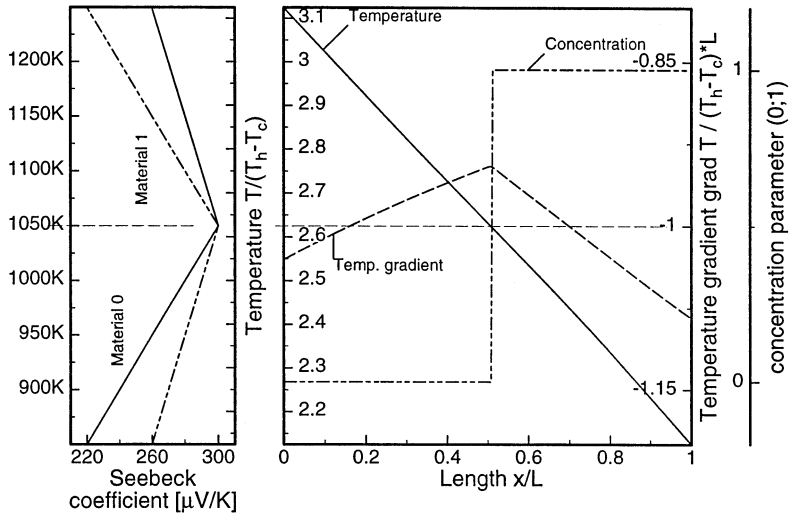

Fig. 3. Calculating the optimum concentration profile in a twofold stacked generator. Provided all other properties are identical, the substance with maximum $|S|$ is selected. The two available $S(T)$ are shown in the left part. Temperature, $T(x)$; temperature gradient, $\nabla T(x)$ and material parameter $c(x)\in\{0, 1\}$ are collected at the right.

The profiles of the material parameters are represented in the same way. E.g.

$$\kappa(x) = \sum_{i,x\in[0,L]} \kappa_i f_i(x), \quad \kappa_i = \kappa(T = T(x = iL/N)).$$

According to the Galerkin method [7,8], a set of equations, that allows the determination of the $\{T_i\}$, is obtained from

$$\int_{x=0}^{L} f_i(x) D([T(x)]) dx \stackrel{!}{=} 0, \quad i = 1 \ldots N \tag{4}$$

With the known functions $f_i(x)$ the integration of Eq. (1) is straightforward.

The transport coefficients S, σ and κ are evaluated, considering the temperature T and the concentration c as independent variables and using the values of the previous step of the iterative calculation of $T(x)$. All derivatives are expressed via the T and c fields:

$$\text{e.g.:} \nabla\kappa = \frac{\partial\kappa}{\partial T}\nabla T + \frac{\partial\kappa}{\partial c}\nabla c. \tag{5}$$

Thus the material parameters S, σ and κ and their derivatives can easily be interpolated from tables $S(T, c)$, $\sigma(T, c)$, and $\kappa(T, c)$, that are given to this routine as input files. We consider this a simpler way than eliminating the temperature or concentration parameter using analytical relations [3,5].

Since Eq. (1) is of second order, a quadratic set of relations between the coefficients $\{T_i\}$ is obtained from Eq. (4). For one-dimensional $T(x)$, as considered here, one single equation for T_{i+1} needs to be solved, once T_{i-1} and T_i are known, or equivalently T and ∇T at one boundary. The corresponding quadratic equation and the appearing coefficients are given below for the general case of temperature and concentration dependent $S(T, c)$, $\sigma(T, c)$ and $\kappa(T, c)$.

$$0 = T_{i+1}^2 \cdot h_1 + T_{i+1}(h_2 + h_3 T_i) + (h_4 T_i^2 + h_5 T_i + h_6 T_i T_{i-1} + h_7 T_{i-1}^2 + h_8 T_{i-1} + h_0), \tag{6}$$

where

$$h_0 = i^2\left(\frac{1}{6}(\rho_{i-1} + \rho_{i+1}) + \frac{2}{3}\rho_i\right);$$

$$h_1 = \frac{1}{6\mathrm{d}x^2}\left(\left.\frac{\partial\kappa}{\partial T}\right|_{i+1} + 2\left.\frac{\partial\kappa}{\partial T}\right|_i\right) + \frac{i}{12\mathrm{d}x}\left(\left.\frac{\partial S}{\partial T}\right|_i + \left.\frac{\partial S}{\partial T}\right|_{i+1}\right);$$

$$h_2 = \frac{\kappa_i}{\mathrm{d}x^2} + \frac{i}{12\mathrm{d}x}\left(\left.\frac{\partial S}{\partial c}\right|_i c_{i+1} - \left.\frac{\partial S}{\partial c}\right|_i c_i + \left.\frac{\partial S}{\partial c}\right|_{i+1} c_{i+1} - \left.\frac{\partial S}{\partial c}\right|_{i+1} c_i\right) + \frac{1}{6\mathrm{d}x^2}\left(-2\left.\frac{\partial\kappa}{\partial c}\right|_i c_i + 2\left.\frac{\partial\kappa}{\partial c}\right|_i c_{i+1} - \left.\frac{\partial\kappa}{\partial c}\right|_{i+1} c_i + \left.\frac{\partial\kappa}{\partial c}\right|_{i+1} c_{i+1}\right);$$

$$h_3 = \frac{i}{6\mathrm{d}x}\left.\frac{\partial S}{\partial T}\right|_i - \frac{1}{3\mathrm{d}x^2}\left(2\left.\frac{\partial\kappa}{\partial T}\right|_i + \left.\frac{\partial\kappa}{\partial T}\right|_{i+1}\right);$$

$$h_4 = \frac{1}{6\mathrm{d}x^2}\left(\left.\frac{\partial\kappa}{\partial T}\right|_{i+1} + 4\left.\frac{\partial\kappa}{\partial T}\right|_{i} + \left.\frac{\partial\kappa}{\partial T}\right|_{i-1}\right) + \frac{i}{12\mathrm{d}x}\left(\left.\frac{\partial S}{\partial T}\right|_{i-1} - \left.\frac{\partial S}{\partial T}\right|_{i+1}\right);$$

$$h_5 = \frac{-2\kappa_i}{\mathrm{d}x^2} + \frac{i(-\partial S/\partial c|_{i-1}\, c_{i-1} + \partial S/\partial c|_{i-1}\, c_i - 3\,\partial S/\partial c|_i\, c_{i-1} + 3\,\partial S/\partial c|_i\, c_{i+1} - \partial S/\partial c|_{i+1}\, c_i + \partial S/\partial c|_{i+1}\, c_{i+1})}{12\mathrm{d}x}$$
$$+ \frac{(-\partial\kappa/\partial c|_{i-1}\, c_{i-1} + \partial\kappa/\partial c|_{i-1}\, c_i - 2\partial\kappa/\partial c|_i\, c_{i-1} + 4\partial\kappa/\partial c|_i\, c_i - 2\partial\kappa/\partial c|_i\, c_{i+1} + \partial\kappa/\partial c|_{i+1}\, c_i - \partial\kappa/\partial c|_{i+1} c_{i+1})}{6\mathrm{d}x^2};$$

$$h_6 = \frac{-1}{6\mathrm{d}x^2}\left(\left.\frac{\partial\kappa}{\partial T}\right|_{i-1} + 2\left.\frac{\partial\kappa}{\partial T}\right|_{i}\right)\frac{i}{6\mathrm{d}x}\left.\frac{\partial S}{\partial T}\right|_i;$$

$$h_7 = \frac{1}{6\mathrm{d}x^2}\left(\left.\frac{\partial\kappa}{\partial T}\right|_{i-1} + 2\left.\frac{\partial\kappa}{\partial T}\right|_{i}\right) - \frac{i}{12\mathrm{d}x}\left(\left.\frac{\partial S}{\partial T}\right|_{i} + \left.\frac{\partial S}{\partial T}\right|_{i-1}\right);$$

$$h_8 = \frac{1}{\mathrm{d}x^2}\kappa_i + \frac{i}{12\,\mathrm{d}x}\left(\left.\frac{\partial S}{\partial c}\right|_{i-1} c_{i-1} + \left.\frac{\partial S}{\partial c}\right|_{i-1} c_i - \left.\frac{\partial S}{\partial c}\right|_{i} c_{i-1} + \left.\frac{\partial S}{\partial c}\right|_{i} c_i\right)$$
$$+ \frac{1}{6\mathrm{d}x^2}\left(\left.\frac{\partial\kappa}{\partial c}\right|_{i-1} c_{i-1} - \left.\frac{\partial\kappa}{\partial c}\right|_{i-1} c_i + 2\left.\frac{\partial\kappa}{\partial c}\right|_{i} c_{i-1} - 2\left.\frac{\partial\kappa}{\partial c}\right|_{i} c_i\right).$$

(c concentration parameter, $\mathrm{d}x = L/N$)

With the aid of this algorithm it is possible to determine the temperature field inside any given generator leg under operation, if S, κ, ρ are known (i.e. tabulated) functions of temperature, and concentration if desired.

Once having obtained the temperature field for a given condition, i.e. material distribution and electric load, it is straightforward to determine all generator characteristics. For example, the internal resistance is calculated by integrating the temperature dependent resistivity along the known temperature profile; the specific output power is given by the electrical current and the load resistance; and to receive the efficiency one additionally calculates the heat flow input by evaluating the temperature gradient at the hot side. For the sake of simplicity an average value for the gradient and the temperature are taken as boundary conditions in the first step. The gradient is varied until the cold junction temperature is matched. Since all thermoelectric effects are in the order of 10% (efficiency) or less, the normalised difference between the temperature field with and without thermoelectric effects ($i = 0$) is expected to be of the same order of magnitude. Therefore a starting value of $i = 0$ is chosen, to calculate a first approximation for $T(x)$. This temperature field is used to calculate the next order value for i. The procedure is iterated until the electrical current as well as the temperature field have stabilised. We have not experienced any trouble concerning convergence.

We implemented the calculus on a standard PC using C++ programming. The demands on computational resources for ~ 100 nodes are still low. An example calculation will be given in Section 6.

The additional concentration parameter so far only serves to introduce different temperature dependencies at different places resembling a certain, fixed material. In the next section we will show how to select that particular material that maximises the electrical power output.

3. Spatial material selection

To maximise the power output or efficiency of a thermoelectric generator, one has to make a choice between different materials at each place. The efficiency of a device is defined as

$$\eta \equiv \frac{P_{\mathrm{el}}}{\boldsymbol{Q}_{\mathrm{in}}}, \tag{7}$$

(P_{el}, electric power output; $\boldsymbol{Q}_{\mathrm{in}}$, total amount of energy/heat flow supplied to the generator at the hot junction.) Consider a stacked generator of M different materials. If there are N slices, the optimum design has to be selected among M^N different candidates. Such procedures have been employed by Anatychuk et al. [9], but for large M and N, approaching continuous grading, this becomes intractable and a well founded criterion for material choice is needed.

We only consider the power output here, because this quantity is to be maximised in most applications of generators.

For an arbitrary generator, the power is given by the difference between outgoing and incoming electric energy flux, $\mu\boldsymbol{j}$. (The complete flux of internal energy is: $\boldsymbol{u} = T\boldsymbol{s} + \mu\boldsymbol{j}$)

$$P_{\mathrm{el}} = \int_{\mathrm{incoming}} \mu\boldsymbol{j}\cdot\mathrm{d}\boldsymbol{A}_i + \int_{\mathrm{outgoing}} \mu\boldsymbol{j}\cdot\mathrm{d}\boldsymbol{A}_0$$
$$= \oint_{\mathrm{surface}} \mu\boldsymbol{j}\cdot\mathrm{d}\boldsymbol{A}$$
$$= \int_{\mathrm{volume}} \mathrm{div}(\mu\boldsymbol{j})\mathrm{d}V. \tag{8}$$

To evaluate Eq. (8), the conservation of charge carriers, $\dot{n}=0 \Leftrightarrow \mathrm{div}\boldsymbol{j}=0$, and the representation of the particle flux, $\boldsymbol{j}=\sigma/e^2(S\nabla T-e\nabla\mu)$ [6], are used. As in the previous Section, the generator is considered to be one dimensional with a cross sectional area A.

$$P_{\mathrm{el}}=\int_{\mathrm{volume}} \boldsymbol{j}\left(\frac{-e^2}{\sigma}\boldsymbol{j}+eS\nabla T\right)\mathrm{d}V \tag{9}$$

$$=A\int_{x=0}^{L}\mathrm{d}x(\underbrace{e\boldsymbol{j}S\nabla T-e^2\boldsymbol{j}^2\rho}_{\equiv\pi_{\mathrm{el}}})$$

$$=Ae\boldsymbol{j}\int_{T_h}^{T_c}\mathrm{d}T\,S-Ae^2\boldsymbol{j}^2\int_0^L\mathrm{d}x\,\rho. \tag{10}$$

This shows that the total electric power output P_{el} can be written as a volume integral over a local contribution π_{el}. Therefore, the maximum power condition is satisfied, if the integrand is maximised in every place. This is possible only, if the particle flux $\boldsymbol{j}$ is known. It can be obtained from basic thermodynamics: The potential μ is related to the electrostatic potential ϕ by $\Delta\mu=-e\Delta\phi$. In an external load circuit (with resistance R) the current is given by $I=\Delta\phi/R=-e\boldsymbol{j}A$. Thus $\Delta\mu=e^2\boldsymbol{j}AR$. On the other hand

$$\Delta\mu=\int_{x=0}^{L}\mathrm{d}x\,\nabla\mu=-e^2\boldsymbol{j}\int_0^L\mathrm{d}x\,\rho-e\int_0^L\mathrm{d}x\,S\nabla T.$$

$$\Rightarrow\boldsymbol{j}=\frac{\int_0^L\mathrm{d}x\,S\nabla T}{e\left(R+\int_0^L\mathrm{d}x\,\rho\right)}. \tag{11}$$

To achieve maximum power output of a power supply, which exhibits constant EMF, independently of the current flow, the external load resistance R must match the requirement $\mathrm{R}=\int_0^L\mathrm{d}x\,\rho$. This holds true for fixed hot and cold side temperature. The right hand side of Eq. (11) is thus determined. With the $\boldsymbol{j}$ value obtained, the choice of maximum π_{el} at every position maximises the output power.

π_{el} contains the integral quantity $\boldsymbol{j}$, that characterises the environment, not only the material. This is indeed a new fact in comparison with selection rules that are based on a 'local figure of merit', $Z=(S^2\sigma)/\kappa$, employing (temperature dependent) local properties.

Practically, it can be checked in simple cases that a material selection based on Eq. (10) does reproduce the expected results: Consider two materials with equal and constant thermal and electric conductivity. The Seebeck coefficient of one species may rise with temperature stronger than the other. They are at the same level at a certain temperature T_e. The first term in Eq. (10) is maximized, by choosing the material with maximum $|\mathrm{S}|$. The second term doesn't change with the material selection, if $\rho(T)$ is constant. Maximising π_{el} according to Eq. (10) is to select the material with maximum $|\mathrm{S}|$, i.e. an interface between both substances is thus to be placed at temperature T_e. As soon as ρ actually depends on T, both terms in Eq. (10) have to be considered. Then, the developed numerical method is necessary for fixing the material interface temperature.

We implemented a computer code to select optimum materials in a given temperature field. This module was combined with the algorithm to determine $T(x)$. In this way a software tool has been designed, that gives the layout of one thermogenerator leg to produce maximum electric power at fixed thermal boundary conditions.The algorithm follows the sequence below:

1. Choose an initial profile of the concentration parameter and select the thermal boundary conditions, T_h and T_c.
2. Choose external resistance.
3. Calculate the temperature field.
4. Using the temperature field of 3. and the overall current related to it, select the optimum concentration parameter at all places.
5. Check whether the concentration and/or temperature have changed significantly. If not: quit, else continue at 2.

We experienced only two or three loops to establish a final concentration field of three stacked materials in a stack of some hundred slices. Altogether this allows to make detailed suggestions on the design of graded or stacked thermoelectric generators with comparably little computational effort.

4. Continuous and discontinuous material changes

So far the concentration parameter c has been treated as a floating real number. This is adequate for problems, where c describes a dopant concentration as may be in $FeSi_2$:Co (see example 4 in Section 6), or the composition of a matrix like in Ge_xSi_{1-x}. Here one intends to create a smooth transition or concentration profile.

The situation is different in stacked generators. Provided no complications arise at the junction, it is possible to combine a high temperature material, e.g. $Ge_{0.3}Si_{0.7}$, with medium temperature material, e.g. PbTe, to increase the accessible temperature interval. In this case, one asks for the best position of the interface. Of course, one imagines a stepwise material transition for which the basic representation of $c(x)$, as given in Eq. (3), is not appropriate. We have chosen another possible form of the concentration profile for this case. Instead of the linear element functions in Eq. (3), constant elements are used:

$$c(x)=\sum_{i,x\in[0,L]}c_i\,g_i(x).$$

$$\text{where } g_i(x)=\begin{cases}0, & \text{if } x\notin[iL/N,(i+1)L/N[,\\ 1, & \text{if } x\in[iL/N,(i+1)L/N[.\end{cases} \tag{12}$$

(L, overall length of the leg, N, total number of elements).

This alters the integrals of Eq. (4). They have to be re-evaluated with $g_i(x)$ instead of $f_i(x)$, and the corresponding Eq. (6) changes. But again a quadratic equation for the determination of T_{i+1} is received, that has the following form:

$$a \cdot T_{i+1}^2 + b \cdot T_{i+1} + c = 0,$$

where a, b, c are still products of material properties, evaluated employing the T field of the previous step, and powers of the temperature coefficients T_i and $T_{i\text{-}1}$. Thus the subsequent determination of the temperature field is not changed.

The selection procedure to determine the 'best' material in each place is not affected by the choice of continuous or discontinuous material changes. Using linear element functions in the representation of $c(x)$, the material properties will vary linearly. So no extreme can occur between two successive tabulated values. The maximum value of π_{el} in Eq. (10) will always be reached at one of the filed values of the concentration parameter c. Obviously the same holds true in case of a stepwise constant $c(x)$, using Eq. (12).

Even though we allow for stepwise material changes, the optimum position of the interface is only determined to a resolution of $2L/N$, not L/N as one might have expected. The reason for this is to be seen in the spatial dependency of the variations in S and κ: Consider a stepwise change in κ at a given temperature T_{step}. Unless a node accidentally happens to fall to a position where $T = T_{step}$, $\partial\kappa/\partial T = 0$ for all nodes. Hence there is no contribution from the terms regarding derivatives of S or κ; in Eq. (6) at all nodes. This problem has to be overcome by further manipulation to the temperature T_{i+1} calculated from Eq. (6). The local conservation of heat flux has to be checked explicitly. In case the incoming heat flux, $-\kappa\,(T_i - T_{i-1})/\mathrm{d}x$, does not match the outgoing flux $-\kappa\,(T_i - T_{i-1})/\mathrm{d}x$, one can conclude, that a stepwise change of κ or S has taken place. The corresponding value of T_{i+1} is adjusted appropriately. Because two neighbouring temperature differences are considered, the spatial resolution for a stepwise change of conductivity is decreased to $2\mathrm{d}x$.

5. Assessment as design tool

5.1. Flexibility of approach

The combination of the finite element calculation of the temperature field under operating conditions and the compatible choice of the optimum material, maximising the local power contribution π_{el}, gives a flexible and easy to use numerical tool. It allows to assess the performance of existing devices and may be used as a design tool when looking for optimised dopant profiles in continuously graded devices or the best interface position of stacked generator legs, incorporating any material properties desired.

This tool may be compared to a different one suggested by Mahan [3]: Instead of the representation of S, σ, and κ as functions of T and c, he eliminates the concentration parameter and chooses σ as independent, $S = S(T, \sigma)$, $\kappa = \kappa(T, \sigma)$, by using the Price relations, [10]. After applying his procedure the back transformation $\sigma(x) \rightarrow c(x)$ has to be done to receive a concentration profile, if desired as design parameter. The calculus proceeds by expanding $\sigma(x)$ as series of Legendre polynomials. Similar to the approach presented here, first a temperature field for fixed $\sigma(x)$ is derived by variation of the temperature gradient at one boundary to match the other boundary temperature.

As in this work, the determination of $T(x)$ is part of an outer loop to find the optimum σ profile. Since in Ref. [3] efficiency, not power, is maximised, the integral value of the efficiency is directly used to decide whether the σ profile has converged or not. No local physical criterion is used, see Section 3.

5.2. Numerical effort

Employing our approach, the determination of the interface position in a stacked generator is possible with a relative precision of $2/N$, N number of nodes, see Section 4. Decreasing the uncertainty thus results in an increased numerical effort growing linearly with N. This holds true for both, continuous and stepwise material changes, since only the representation of $c(x)$ is changed, not the structure or number of equations to be solved.

In Ref. [3] it is claimed that only two Legendre terms are required for a fair representation of $\sigma(x)$. In this case continuous grading is considered and the computational demands should be extremely low: For each determination of a T field only the algebraic relations $S(T, \sigma)$, $\kappa(T, \sigma)$ have to be evaluated as well as a coupled set of two equations for the two Legendre coefficients.

The representation of a discrete junction is more complicated: To achieve the same resolution as with the finite-element approach employing N nodes, the number of Legendre terms required is of order N. Solving for the Legendre coefficients results in N equations with roughly N terms each. Thus the numerical effort increases with the order of N^2. Questions how to derive the individual coefficients from these equations are not even considered in this estimate.

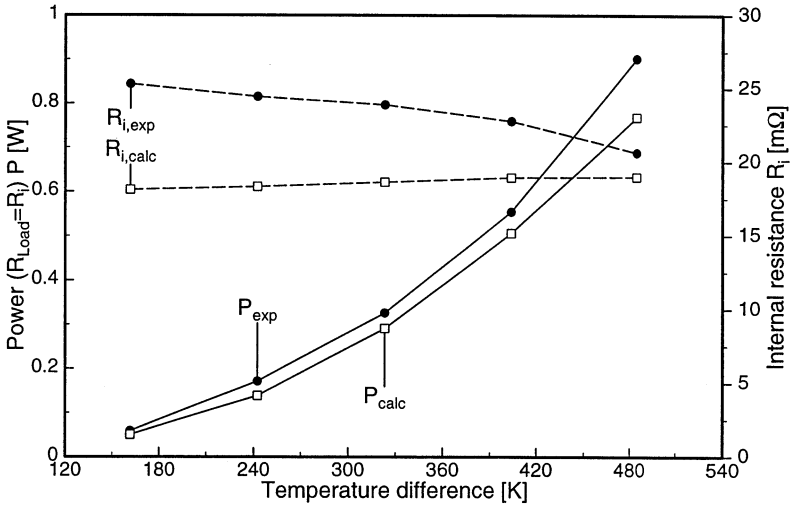

Fig. 4. Recalculation (subscript **calc**) of the device performance of a $FeSi_2$ generator analysed in Refs [12,13] (subscript **exp**). The simulation neglects the finite electric resistance of the hot junction, thus the calculated values of the internal resistance are lower than the experimental ones.

5.3. Describing different materials

Another interesting difference between Ref. [3] and this approach results from the usage of the Price relation [10], in Mahan's paper. The empirical relations $S = S(T, \sigma)$ and $\kappa = \kappa(T, \sigma)$, will allow to cover a variety of materials and dopants. They use two free coefficients, the energy gap and a scattering parameter, that may be chosen for each material. But still there is no physical need for these relations to be generally valid. Forthcoming materials, e.g. quantum well materials for S enhancement, should require additional free parameters to find equivalent relations. Even classical counter doped material will not fit into the Price scheme as soon as the temperature allows both dopants to be significantly activated (since there is just one parameter for the energy gap).

Regarding this, the use of Price relations or similar ones for different material classes will always pose limitations on the 'allowed' σ interval. As soon as the calculus of Ref. [3] suggests values beyond this range, the output is no longer useful as information for device designers. We consider our approach superior in this point: The input data are filed tables of S, σ, and κ versus T, c. The material choice is restricted to the filed values and can be regarded as a choice between existing, tested and desired materials. The treatment of new, non-classical materials is easily included, once the dependencies $S(T, c)$, $\sigma(T, c)$, and $\kappa(T, c)$ are known.

6. Results

It is difficult to obtain reliable data on the performance of thermoelectric materials for different 'concentration parameters', like dopant concentrations or matrix composition. So at this stage we restrict ourselves to four cases: (1) Calculation of the temperature field for one single material. (2) Determination of the temperature field in a stacked generator. The different materials are characterised in adjacent temperature intervals. The temperatures for the material changes are thus fixed and this allows to treat this configuration as one material with stepwise changing properties, skipping the selection procedure. (3) Selection of one out of two materials with maximum Seebeck coefficient. (4) Simulation of experimentally derived performance.

1. First we prove that this approach allows to calculate reliable temperature fields. Sherman et al. [4], have established a numerical procedure to determine the performance of thermoelectric devices. We have chosen their example II for power generators for a comparison. The temperature profiles are indeed very close to each other. Subsequently all other performance data coincide. We could obtain no original numerical data sets from their work, so we digitised their published diagrams. Nevertheless a deviation of $\leq 1\%$ is found for the local temperature. Within the limits of the possible precision we consider this conformity perfect. Our results for the n-leg are compared to the data of Ref. [4] in Fig. 2.

2. In the work of Swanson et al. [11] the design for a stacked generator is discussed. They assume fixed temperatures for the material changes and proceed as follows: The interface positions between successive materials are determined by considering the net heat fluxes and the electric output power. Concerning conduction of heat, a linear temperature profile is assumed in each segment, neglecting distortions due to Joule and Thomson heats as well as temperature dependence of thermal conductivity. We found the interface positions directly

from the temperature profiles. The stepwise changes of material properties at the given interface temperatures cause the temperature gradient to be discontinuous. The interface positions are located at these discontinuities. Since here the fully non-linear temperature profile is included, slight deviations between Ref. [11] and our work are expected. A fair coincidence of both approaches is summarised in Table 2.

3. The selection of the 'best' material is demonstrated in a simple situation. A stacked generator leg of two materials is considered. Both species have identical, constant electrical and thermal conductivity. The variation of the Seebeck coefficient with temperature is shown in the left diagram of Fig. 3. The concentration parameter changes abruptly from one material to the other at a certain position. The corresponding interface temperature is depicted in Fig. 3. One finds that the procedure locates the interface exactly at the temperature where both materials have the same Seebeck coefficient. The material with the maximum magnitude of S is selected, as one has expected.

4. The group of Birkholz has published detailed experimental results on the performance of their generators [12,13]. In these works, a cylindrical $FeSi_2$-generator is analysed. p and n-leg are connected by a bridge of sintered $FeSi_2$ of 2.5 mm thickness. The individual legs have a length of 10.5 mm each. In our calculation we assumed an ideal hot junction showing no thermal and electrical resistivity. The material properties were only documented for the n-material, $FeSi_2$:Co [14]. $FeSi_2$:A1 similar to the p-material used in Refs [12,13] was analysed by Hesse [15]. Since the measurement of thermoelectric properties is difficult in any case and sensitive to the very material under consideration, the agreement between experimental and calculated performance data is very satisfactory. Differences in the resistance can be ascribed to the electrical junction resistance, which is neglected in our calculation Fig. 4.

These examples clearly show that the calculation of the temperature field performs well. The subsequent choice of optimum concentration profiles is harder to judge [16]. But the simple tests presented here, reproduce classical results exactly and the recalculation of available studies on stacked generators gives satisfying agreement. Though not using the material selection procedure, the simulation of experimental data on whole generators shows the flexibility and reliability of this calculus.

Acknowledgements

The work was supported by the Deutsche Forschungsgemeinschaft (DFG) within the 'Graduiertenkolleg Schmelze, Erstarrung, Grenzflächen', (L.H.) and a research project on 'Functionally Graded Materials (FGM)'.

References

[1] H.J. Goldsmid, in: D.M. Rowe (Ed.), CRC Handbook of Thermoelectrics, chapter 3, CRC Press, Boca Raton, 1995.
[2] A.F. Joffe, Pat. USSR No. 126 158, Byulleten' izobretenii (Invention Review) 4 (1960) 22.
[3] G.D. Mahan, J. Appl. Phys. 70 (1991) 4551.
[4] B. Sherman, R.R. Heikes, R.W. Ure, J. Appl. Phys. 31 (1960) 1.
[5] J. Teraki, T. Hirano, in: I. Shiota, Y. Miyamoto (Eds.), Proc. of the 4. Int. Symp. on Functionally Graded Materials (FGM'96), Tsukuba, Japan, in Functionally Graded Materials 1996, Elsevier, Amsterdam, 1997, p. 483.
[6] C.A. Domenicali, J. Appl. Phys. 25 (1954) 1310.
[7] K.J. Bathe, Finite Element Procedures in Engineering Analysis, Prentice Hall, Englewood Cliffs, NJ, 1982.
[8] O.C. Zienkiewicz, The finite element method, McGraw-Hill, NY, 1977.
[9] L.I. Anatychuk, L.N. Vikhor, in: I. Shiota, Y. Miyamoto (Eds.). Proc. of the 4. Int. Symp. on Functionally Graded Materials (FGM'96), Tsukuba, Japan, in Functionally Graded Materials 1996, Elsevier, Amsterdam, 1997, p. 501.
[10] P.J. Price, Phys. Rev. 104 (1956) 1223.
[11] B.W. Swanson, E.V. Somers, R.R. Heikes, Trans. ASME: J. Heat Transfer 83 (1961) 77.
[12] U. Birkholz, E. Groß, U. Stöhrer, in: D.M. Rowe (Ed.), CRC Handbook of Thermoelectrics, chapter 24, CRC, Boca Raton, 1995.
[13] U. Stöhrer, R. Voggesberger, G. Wagner, U. Birkholz, Energy Convers. Manag. 30 (2) (1990) 143.
[14] U. Stöhrer, PhD thesis, Univ. Karlsruhe (TH), Germany, 1993 (in German).
[15] J. Hesse, Z. Metallkde. 60 (8) (1969) 652 (in German).
[16] J. Schilz, L. Helmers, W.E. Müller, M. Niino, J. Appl. Phys. 83 (1998) 1150.